

30/10-9-86 JS

3 dialh  
(27)

I-28211 CONF-860870--11DR# 1991-7  
SLAC-PUB-4038  
July 1986  
(A)

**LINEAR ACCELERATORS OF THE FUTURE\***

SLAC-PUB--4038

GREGORY A. LOEW

Stanford Linear Accelerator Center

Stanford University, Stanford, California 94305

DE87 000327

**Introduction**

To become feasible within our present scientific, technical and economic perspectives,  $e^+e^-$  colliders of the future will require linear accelerators of unprecedented efficiency supplied by electron and positron bunches of unprecedentedly small emittance focused to interaction points of unprecedentedly small cross-section. The purpose of this paper is to review some of the requirements imposed on these linear accelerators and some of the approaches that are presently being examined. Figure 1 shows on the left the first member of this new generation of machines to which it will be useful to compare the "generic"

linear collider of the future, shown on the right with all its essential elements. The layout of the "generic" machine has the advantage that it avoids the beam dynamics complications and the synchrotron energy loss of the arcs which were necessary to fit the SLC on the SLAC campus. Figure 2 shows along the left-hand scale the approximate luminosities required by the event rates expected at the center-of-mass energies to be explored, one and two orders of magnitude above the SLC. The points corresponding to VEPP I ( $e^+e^-$ ), to the SSC (pp) and to the approximate  $e^+e^-$  equivalent range are also shown.

**BUILDING BLOCKS FOR  $e^+e^-$  LINEAR COLLIDERS**

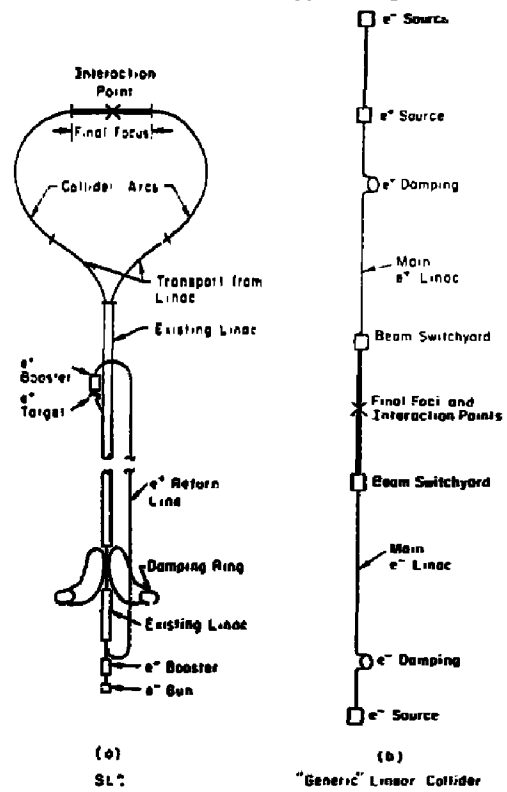


Fig. 1. Building blocks for  $e^+e^-$  linear colliders: (a) SLC; (b) "Generic" linear collider.

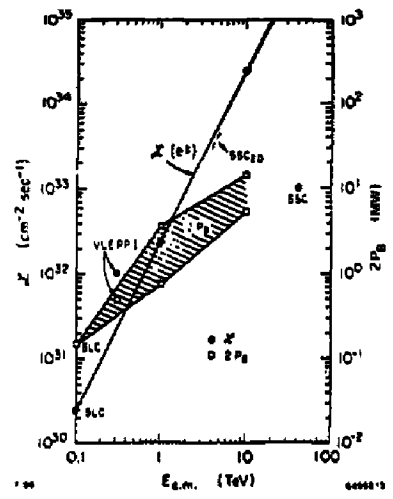


Fig. 2. Required luminosity  $\mathcal{L}$  and average beam power  $2P_B$  as a function of center-of-mass energy,  $E_{c.m.}$ .

**Beam Power**

The now well publicized expressions which relate luminosity  $\mathcal{L}$  to the other beam parameters such as average beam power  $P_B$ , disruption  $D$ , geometric emittance  $\epsilon$ , normalized or invariant emittance  $\epsilon_n$ , beamstrahlung energy spread  $\delta$  ( $\delta_{CL}$  in the classical and  $\delta_{QM}$  in the quantum mechanical regime) and bunch length  $\sigma_z$ , are given below in MRS units for round beams ( $\sigma_x = \sigma_y = \sigma_r$ ):

$$\mathcal{L} = f_r b \frac{N^2}{4\pi\sigma_z^2} H(D) = f_r b \frac{N^2 \gamma}{4\pi\epsilon_n \beta^2} H(D) \quad (1)$$

$$D = \frac{\gamma \epsilon_n N}{\gamma \sigma_z^2} = \frac{\gamma \epsilon_n N}{\epsilon_n \beta^2} \quad (2)$$

$$2P_B = 2 f_r b N \gamma m c e^3 \quad (3)$$

\* Work supported by the Department of Energy, contract DE-A C03-78SF00518.

Invited paper presented to the 13th International Conference on High Energy Accelerators Novosibirsk, USSR, August 7-11, 1986

**MASTER**

THIS DOCUMENT IS UNLIMITED

Table 1. Examples of Beam Parameters for  $E_{c.m.}$  of 0.1, 1 and 10 TeV

$$\delta_{CL} \approx \frac{5 \times 10^{-45} N^2 \sigma_x^2}{\epsilon_n \epsilon_n \beta^*} H(D) \quad (4a)$$

$$\delta_{QM} \approx 7 \times 10^{-9} \left( \frac{N^2 \sigma_x}{\epsilon_n \beta^*} \right)^{1/3} \quad (4b)$$

$$\sigma_r = \left( \frac{\epsilon_n \beta^*}{\gamma} \right)^{1/2} \quad (5)$$

Here  $r_c$  is the classical radius of the electron,  $\gamma$  the normalized  $e^\pm$  energy  $E/\gamma m_0 c^2$ ,  $f_r$  the machine repetition rate,  $b$  the number of bunches per pulse,  $N$  the number of particles per bunch,  $H(D)$  the pinch enhancement factor (which can vary between 1 and 6) and  $\beta^*$  the envelope function at the final focus. Expression (4a) applies when the critical photon energy ( $\hbar\omega_c$ ) is much smaller than  $\gamma m_0 c^2$ . Expression (4b) applies when  $\hbar\omega_c > \gamma m_0 c^2$ . If one makes the beams not "round" but "elliptical" (i.e.,  $\sigma_x \neq \sigma_y$ ) which they probably will be anyway because of inevitable transport astigmatism, one must introduce a factor  $R$  equal to  $\sigma_x/\sigma_y$  into many of the above expressions (for complete expressions, cf Ref. 1). To the extent that this aspect ratio is adjustable, one gains an extra degree of freedom to control the energy spread due to beamstrahlung, at the cost of some added complexity in the design of the final focus. Also note two other points. The first is that the physics of quantum emission during the  $e^\pm$  bunch interaction which results in expressions (4a) and (4b) is still under study. In the transition between the two regimes,  $\delta$  will probably assume the form  $\delta_{CL} H_T(\bar{T})$  where  $\bar{T}$  is a scaling parameter defined by  $\gamma B/B_c$ ,  $B$  is the local magnetic field seen by the particles in the opposing bunch,  $B_c = 4.4 \times 10^9$  T, and  $H_T(\bar{T})$  is a reduction factor ( $\leq 1$ ). This factor which can be obtained from a simulation decreases with increasing  $\bar{T}$ , the latter being the effective value of  $\bar{T}$  over the bunch. The second point is that expression (5) assumes that the final focus system is achromatic to the degree that chromatic effects are negligible.

We can now rewrite the average beam power in several illustrative ways:

$$P_B \approx 10^{-12} \frac{\mathcal{L} \epsilon_n \beta^*}{NH(D)} = 10^{-12} \frac{\mathcal{L} \gamma \sigma_x^2}{NH(D)} \quad (6a)$$

$$P_{B,CL} \approx 7 \times 10^{-35} \mathcal{L} \gamma \left( \frac{\epsilon_n \beta^*}{\sigma_x \delta_{CL} H(D)} \right)^{1/2} \quad (6b)$$

$$P_{B,QM} \approx 0.88 \times 10^{-24} \mathcal{L} \left( \frac{\epsilon_n \beta^* \sigma_x}{\delta_{QM}^3} \right)^{1/2} \quad (6c)$$

Expression (6a) shows that the required average power in the beam is quite independent of the linac design: indeed  $\mathcal{L}$  is imposed by the experimenters,  $\epsilon_n$  is determined by the source, i.e., the injector and/or the damping ring ( $\epsilon_n$  must not be allowed to grow substantially in the linac),  $H(D)$  is due to the "pinch" effect and  $\beta^*$  depends on the focusing strength at the

$E_{c.m.}$ (TeV)	0.1 (SLC)	1	10
$\mathcal{L}$ ( $\text{cm}^{-3} \text{sec}^{-1}$ )	$2.4 \times 10^{30}$	$2.4 \times 10^{31}$	$2.4 \times 10^{34}$
$\beta^*$ (m)	$7.5 \times 10^{-3}$	$7.5 \times 10^{-3}$	$10^{-3}$
$\epsilon_n$ (mrad-m)	$3 \times 10^{-5}$	$1.5 \times 10^{-6}$	$10^{-8}$
$\epsilon_n \beta^*$	$2.25 \times 10^{-7}$	$1.125 \times 10^{-8}$	$7.5 \times 10^{-11}$
$\sigma_r$ ( $\mu\text{m}$ )	1.5	0.1	$0.038$
$N(e^\pm)/\text{bunch}$	$5 \times 10^{10}$	$10^{10}$	$2.4 \times 10^9$
$\sigma_x$ (mm)	1	0.25	$10^{-3}$
$D$	0.63	0.63	1.1
$H(D)$	1.5	1.5	4
$\delta$	$0.8 \times 10^{-3}$	0.266	0.3
$2P_B$ (MW)	0.144	3.6	14.7
$f_r b$	180	2300	3800

final focus. As to the value of  $N$ , it is fixed by expressions (4a) or (4b), once  $\sigma_x$  and  $\delta$  are chosen. The only way that  $N$  can increase above the constraints of (4a) is through the reduction factor  $H_T(\bar{T})$  mentioned above. For energies below 1 or 2 TeV where machines are likely to work in the classical regime,  $\sigma_x$  is in the denominator in both expressions (4a) and (6b) and it is advantageous to work with relatively long bunches and hence long wavelengths. For higher energy machines,  $\sigma_x$  is in the numerator in both expressions (4b) and (6c) and short bunches are mandatory. Using expressions (6b) and (6c) as pointed out by Panofsky,<sup>3</sup> we can get families of curves for the factor  $P_B/\mathcal{L}(\epsilon_n \beta^*)^{1/2}$  versus  $\sigma_x$  for different  $\gamma$ 's and fixed values of  $\delta$  (typically an acceptable maximum of 0.3) in both the classical and quantum mechanical regimes: again, once  $\sigma_x$  is chosen, the above factor is determined. One can then independently play with  $\epsilon_n$  and  $\beta^*$  (as long as  $\beta^* > \sigma_x$ ).

Taking the SLC as a starting point, two consistent sets of parameters at two c.m. energies, 1 TeV and 10 TeV, have been calculated in Table 1. The upper and lower values of  $2P_B$  are plotted in Fig. 2. The points yielding higher beam powers assume weaker final focusing. The values chosen for  $\epsilon_n$  have been selected somewhat arbitrarily as a result of guesses (indeed very optimistic) made by several authors who studied the possibilities of cooling rings as injectors for TeV colliders.<sup>3</sup> The bunch length was selected as a function of an RF wavelength that might be acceptable (see discussion below). The total number of bunches ( $f_r b$ ) and the number  $N$  of  $e^\pm/\text{bunch}$  are not free parameters in this derivation but of course, the higher  $N$ , the lower the necessary  $f_r b$  for a given luminosity. Note also that the luminosities calculated on the basis of these parameters allow for no dilution of  $\sigma_r$  due to energy dispersion, higher order optical effects, vibrations or other deleterious effects.

### Linac Options

Let us now turn to the linacs. Given the values of  $E_{c.m.}$ ,  $2P_B$ ,  $\delta$ ,  $\sigma_x$ ,  $\epsilon_n$ ,  $\beta^*$ ,  $N$  and  $f_r b$  specified above, what must the linacs be able to do? The crucial issues to be considered are the gradient, the related choices of RF frequency (if the linac

uses RF), peak power and energy stored, the wakefields and the number of bunches per pulse. Before we consider these issues in some detail, let us review briefly the linac approaches which are presently being considered. Figure 3 summarizes these in schematic form, to the exclusion of schemes using laser and plasma acceleration which are treated by others at this conference.

Figure 3(a) shows the conventional linac in which individual or sub-groups of accelerator sections are driven by individual RF sources such as pulsed klystrons, gyroklystrons or lasertrons. The pulse length of the RF driver is  $n t_F$  where  $t_F$  is the filling time of the section(s). The peak power of the source is boosted if necessary by an energy compression system which shortens the effective pulse length by the factor  $n$ , and

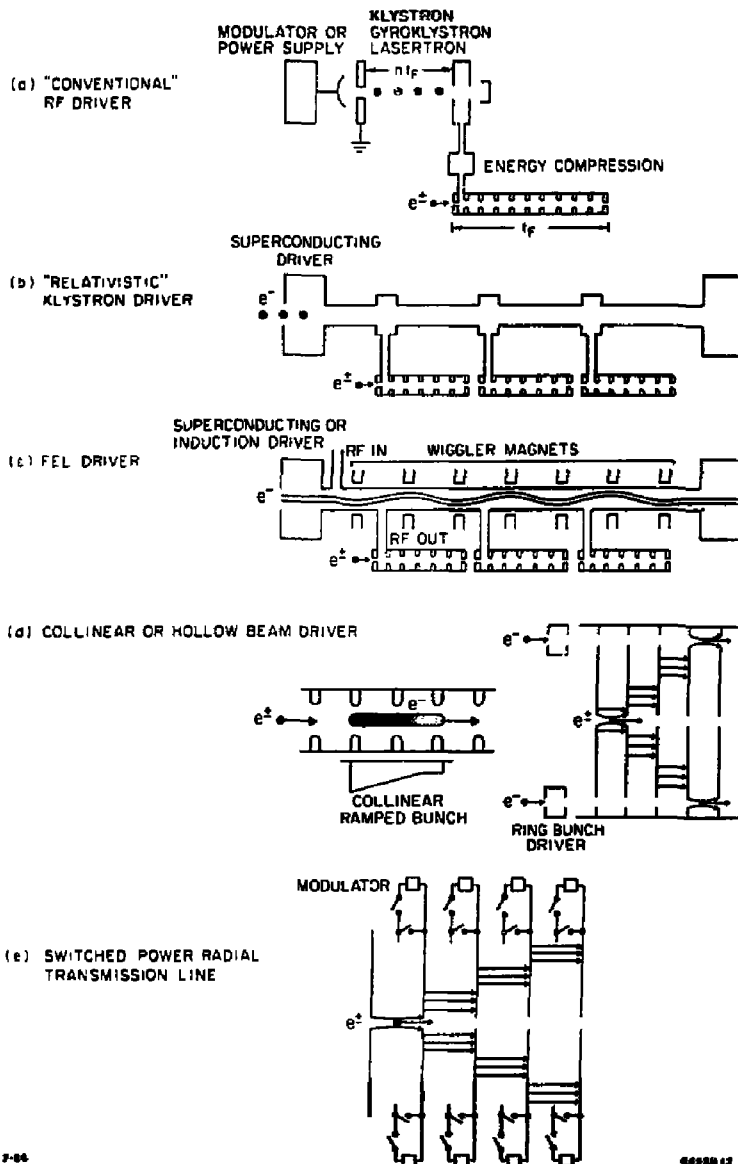


Fig. 3. Various linac options presently under study.

at the cost of some efficiency produces the desired input power to the section. The advantages of this type of linac are well known. In particular, for a multi-section machine, if one source out of many fails, operation is not significantly impaired.

Figure 3(b) shows a scheme where the multiple sources of 3(a) are replaced by one or a few in which a high current, bunched relativistic beam induces power into short cavities (much like the output cavities of klystrons) which in turn feed the linac sections. As the energy of the driving bunches is spent, it has to be replenished. This idea is actually an old one but it has recently been revived by W.K.H. Panofsky, and studied by W. M. Fawley, *et al.*,<sup>4</sup> and W. Schnell.<sup>5</sup> In the latter approach, the driver linac is a relatively low frequency (350 MHz), low gradient (6 MV/m) superconducting machine which produces a 3 GeV train of very short, high current bunches ( $3$  or  $4 \times 10^{11}$   $e^-$  within 1 mm). These bunches drive much higher frequency (20-30 GHz) "transfer" cavities which are the actual high power sources for the linac sections. As they lose energy, the driving bunches are periodically reaccelerated to 3 GeV. Some energy recovery may be possible between the output of each linac section and the subsequent transfer cavity. This overall approach has the advantage that it uses only one gun (or perhaps a few). The efficiency of the scheme is in principle competitive but the overall degradation of the driving bunches due to energy spread and emittance growth remains to be studied. The overall effective gradient of the accelerator is decreased by the length of the superconducting driving linac which inevitably occupies some of the length. Furthermore, if the driving beam is interrupted, the entire installation is down.

Figure 3(c) is a variation of 3(b) in which the RF is generated by free electron laser action of a bunched beam from a superconducting linac or a continuous beam ( $\sim 10$ -20 nsec long) from an induction linac. Either one is caused to wiggle transversely and to deliver energy to the TE<sub>01</sub> fields in an overmoded rectangular guide. This scheme is commonly called the "two-beam accelerator" and has been studied in detail by A. M. Sessler and D. B. Hopkins,<sup>6</sup> and also by U. Amaldi and C. Pellegrini.<sup>7</sup> The LBL group has successfully used the Experimental Test Accelerator (ETA) at Livermore to generate  $\sim 15$  nsec pulses of more than 1 GW of peak power at 35 GHz by passing a 3 kA beam through a tapered undulator. A fraction of this power was used to test a seven-cavity traveling-wave structure up to an accelerating field of 180 MV/m, and more experimental work is underway. The overall FEL approach is certainly very encouraging from the point of view of generating pulses of unprecedented high peak power. Numerical simulations to study the longitudinal properties of the FEL beam as it travels along the waveguide from driver to driver are also encouraging. Much work, however, remains to be done on the potential transverse phase space growth, the generation of sideband power which would degrade efficiency, and on microwave phase sensitivity to frequency, undulator field, beam current and energy. The gradual removal of the microwave power from the rectangular waveguide as it is being generated also remains to be tested carefully. Overall, the same general comments can be made about this approach as for the one under 3(b).

Figure 3(d) is another variation of 3(b) in which very intense single-driving bunches are passed through periodic structures to generate very high wake fields behind them, either collinearly or through a ring beam. This idea was pioneered

by G. A. Voss and T. Weiland,<sup>8</sup> and studied in general by others such as P. B. Wilson.<sup>9</sup> Commonly referred to as a wake field accelerator, this scheme is characterized by a transformer ratio of the maximum accelerating gradient seen by a test charge behind the driving bunch to the maximum retarding field within the driving bunch. The collinear approach, to give a substantial transformer ratio (say 10 to 15), requires a long high-current driving bunch, with typically a quarter-wave front porch and a rising linear ramp, two or three wavelengths long. For a 200 MV/m gradient, the peak current at the end of such a bunch might have to be 10 kA for a 30 GHz slow-wave SLAC-type structure. To sustain these gradients, new driving bunches would have to be injected or reaccelerated every ten meters. How such bunches would be generated and shaped has not yet been studied in detail. On the other hand, the hollow or ring bunch approach is presently under intense study at DESY. It benefits from the radial inward flow of the pulsed energy after it has been generated on the annular rim of the structure, and results in field strengths varying roughly as  $r^{-(1/2)}$ . In the DESY experiment, a laser-driven gun produces a high current (1 kA, 150 keV) hollow ring which is accelerated by a 500 MHz linac to 8 MeV and bunched to a length of 1 cm or less. A transformer ratio of ten is expected. For a bunch length of 0.5 cm of charge 1  $\mu$ C, the axial accelerating field has been calculated to yield 100 MeV/m. The wakefield accelerator is an interesting scheme from which much will certainly be learned but several problems remain to be studied in detail such as bunch generation, shaping and stability, possible radial asymmetries resulting in severe transverse deflecting wake fields on axis, and the lack of space near the axis to locate focusing quadrupoles for the accelerated bunch which must not affect the driving bunch. Also, it is not clear that the short wake field pulses will be available for more than one or two bunches before the wave packets bounce back and forth and lose amplitude by phase decoherence between modes.

Figure 3(e) is similar to the previous ring wake field accelerator except that the driving bunch is replaced by an array of charged annular ring capacitor plates. These are successively charged by external modulators and discharged very rapidly to create the same radial transmission line effect in which the inward traveling axial energy and field are enhanced by some ratio  $R$  which depends on the disk outer radius, the gap width and the switching rise time. This approach has been pioneered by W. Willis<sup>10</sup> at CERN and is under study jointly with R. Palmer, I. Stumer *et al.*, at Brookhaven. This so-called switched power linac uses distributed photodiodes driven by short pulses of laser light. The accelerating structure consists of copper disks, 6 cm in radius with a disk spacing of 1 mm and a disk thickness of 0.6 mm. The photodiode gap at the rim is 0.5 mm and is charged to 40 kV. Upon inward flow of the energy towards the inner radius of 0.5 mm, the accelerating field pulse is calculated to reach 1.6 GV/m with an average gradient of 1 GV/m. The laser can be pulsed once, or several times in a row to produce a multi-pulse buildup. Energy recovery might be possible if the reflected pulse, after passage of the accelerated beam, is reabsorbed by a second photodiode switch on the opposite side of the gap. A variation of this scheme has been proposed by F. Villa<sup>11</sup> at SLAC in which the disks are charged by means of Marx generators and Blumlein lines up to 230 kV, and the discharge is caused by a laser triggering an electron avalanche discharge in an argon high pressure gap.

With a gap spacing of 1.5 mm, an axial gradient of 1.5 GeV/m is calculated. An efficiency as high as 65% to bring the energy from the AC to "storage" on axis of the linac might be achieved. Because these approaches could be very efficient, their study should be encouraged even though they suffer from some of the disadvantages of the wake field accelerator with respect to transverse wake fields and lack of space for focusing quadrupoles, in addition to their own generic difficulties regarding laser focusing and switching.

### Linac Parameters

One way to look at all the above schemes is that at the time of passage of the bunch to be accelerated, the structure looks like two parallel circular capacitor plates with coaxial holes, across which there is a given electric field gradient  $G$  and a total energy stored per unit length  $W$ . The figure of merit of the structure,  $G^2/W$ , not too surprisingly, has the dimensions of an inverse capacitance or elastance<sup>12</sup> which will be called  $s$ . Let us from here on concentrate on the RF linacs, i.e. any scheme from Figs. 3(a) through 3(c). In this case,  $s$  is related to the shunt impedance per unit length  $r$  and  $Q$ , or to a factor often denoted as  $k_1$ , through the relations

$$s = \frac{\omega r}{Q} = \frac{G^2}{W} = 4k_1 \quad (7)$$

where the parameters  $s$  and  $k_1$  scale as  $\omega^2$  and  $r/Q$  scales as  $\omega$ . The total energy stored per linac of length  $L$  before the beam is injected is

$$\bar{W}L = \frac{\bar{G}^2 L}{s} = \frac{E\bar{G}}{s} \quad (8)$$

where  $\bar{W}$  and  $\bar{G}$  are average values of  $W$  and  $G$  which can vary somewhat over the modular length of the structure depending on pulse shape, loss, beam loading or construction. This simple equation illustrates the central issue of the entire linac design. On the one hand, we would like to minimize the length  $L$  of the machine to economize space, which makes the highest possible gradient  $\bar{G}$  desirable. On the other hand, for a desired particle energy  $E$ , a large value of  $\bar{G}$  implies a high value of  $\bar{W}$ . We will see below that perhaps only a few percent of the energy stored in the structure can be removed profitably by the beam. The rest, unless it can be recovered, is wasted as heat. The beam energy gain per bunch per unit length is given by  $P_B/f_r bL$ , typically 0.16 joule/bunch/meter for the SLC. The energy stored per meter,  $\bar{W}$ , being 5.64 joules, the single bunch efficiency  $\eta_{sb}$  for the SLC is only 2.8%. In general,

$$\eta_{sb} = \frac{N e C \cos \theta_0}{\bar{W}} = \frac{N e s \cos \theta_0}{\bar{G}}$$

where  $\theta_0$  is the average angle at which the bunch rides with respect to the crest. For a SLAC-type structure,  $s = C_0 \omega^2$  V/C-m where  $C_0 = 2.3 \times 10^{-3}$ . [An exact expression as a function of group velocity  $v_g$  is given in Ref. 1, Eq. (3.2).] Thus

$$\eta_{sb} = \frac{N e C_0 \omega^2 \cos \theta_0}{\bar{G}} \quad (9)$$

This expression tells us that for a given  $N$ ,  $\eta_{sb}$  decreases with the gradient but increases as  $\omega^2$ . Thus if we increased the SLC gradient by a factor of 10 (200 MV/m) but increased the frequency by a factor of 3 or perhaps 4, nothing much would

be changed. We see however from Table 1 that  $N$  in the future machines is lower by a factor of 10 or even 100. Hence only two avenues are open: either one must increase the frequency by yet another order of magnitude or one must learn how to accelerate many bunches per RF pulse to increase the efficiency to  $b\eta_{sb}$ . We will come back to this point at the end of the article.

What do we know about permissible gradients? Figure 4 summarizes the present experimental and theoretical state of knowledge over a wide range of wavelengths. Three different regimes are shown. The lowest range is determined by electrical breakdown. The experimental points were obtained recently in a short RF structure<sup>13</sup> or in half-cavities.<sup>14</sup> The maximum surface fields were actually twice as high, i.e., several times above those given by the Kilpatrick criterion. The variation of breakdown gradient seems to go roughly as  $\omega^{0.5}$ , somewhat slower than predicted by others<sup>15</sup> (i.e.,  $\omega^{7/8}$ ). This could be because our experiments were conducted over a narrow range of pulse lengths, i.e.,  $\sim 1-3$   $\mu$ sec, whereas at higher frequencies, the RF pulses would be much shorter (varying as  $\omega^{-3/2}$ ) and the probability of breakdown might be reduced. Above a wavelength of 1 mm (i.e., 300 GHz), surface melting due to heating in two successive regimes ( $\omega^{1/8}$  and  $\omega^{1/4}$ ) takes over. If we believe these results, at 30 GHz one should be able to operate at 500 MV/m. Note however<sup>13</sup> that the S-band cavity measurements at 150 MV/m were accompanied by very large field emission currents, and that at 120 pps operation, close to 0.75 megarad per hour of X-ray radiation was present on the side of the structure. Clearly, caution will have to be taken that the field emitted current during the pulse does not become comparable to the current to be accelerated.

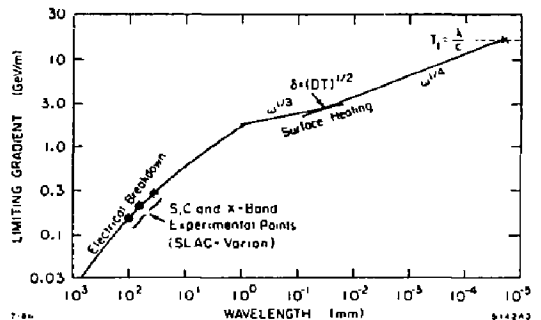


Fig. 4. Limiting accelerating gradient as a function of RF wavelength.

Let us now turn to the issue of energy storage and peak power. Due to lack of space in this paper, the reader is referred to Ref. 16 for a detailed discussion of the advantages of traveling-wave (TW) versus standing-wave (SW) structures, as well as constant-impedance (CI) versus constant-gradient (CG) structures. The general conclusion is that the choice is not crucial from an electrical point of view and that the selection will probably be made on the basis of mechanical criteria, ease of fabrication, and economics. Using the equations for a TW, CG structure, the attainable voltage per section of length  $l$ , input power  $P$  and filling time  $t_F$ , the RF energy needed per pulse, the efficiency of storing this energy and the peak power needed

per unit length are given by:

$$V = (1 - e^{-2r})^{1/2} (Pr\ell)^{1/2} \quad (10)$$

$$P_{TP} = \left( \frac{2r}{1 - e^{-2r}} \right) \frac{V^2}{\ell} \quad (11)$$

$$\eta_{ST} = \frac{1 - e^{-2r}}{2r} \quad (12)$$

$$\frac{P}{\ell} = \frac{G^2}{r} \frac{1}{1 - e^{-2r}} \quad (13)$$

where  $r$  is the attenuation of the section ( $\omega\ell/2v_p Q$ ) and  $t_F$  is the filling time ( $2Qr/\omega$ ). Referring to Fig. 5, we see that there is a trade-off between  $\eta_{ST}$  and normalized  $P/\ell$ : at large  $r$ ,  $\eta_{ST}$  is low and  $P/\ell$  is low, and vice versa. Thus storing energy efficiently requires relatively higher peak power.

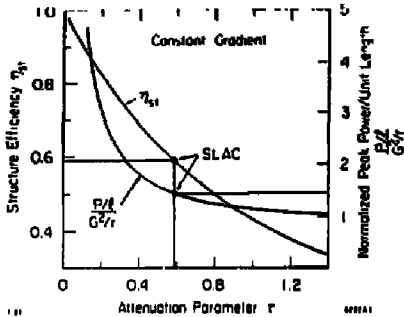


Fig. 5. Structure efficiency and normalized peak power vs.  $r$ .

Another informative way of presenting the data in Eq. (13) is to fix  $r$  (say to 0.50), and to plot  $P/\ell$  and  $t_F$ , as in Fig. 6,

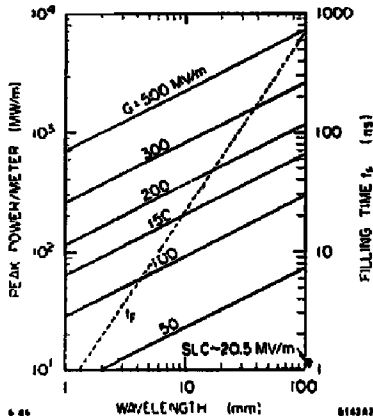


Fig. 6. Peak power per meter and filling time as a function of wavelength for various values of accelerating gradient for a typical disk-loaded structure ( $r = 0.5$ ).

noting that  $r$  varies as  $\omega^{1/2}$  and  $Q$  as  $\omega^{-1/2}$ . We see that in comparison with the SLC where  $P/\ell$  is only 11 MW/m, an accelerator with a 200 MV/m gradient at  $\lambda = 10.5$  cm (2856 MHz) will require over 1100 MW/m, but that at  $\lambda = 1$  cm (the frequency of the LBL two-beam accelerator), this power would be reduced to about 350 MW/m, still a formidable amount of peak power. Obviously, conventional klystrons whose power output drops roughly as  $\omega^{-5/2}$  will not be available for this application unless their voltage or current can be greatly increased. The only other technique available with conventional sources is energy compression either of the SLED type<sup>17</sup> which is only 50% efficient, or of the type<sup>18</sup> shown in Fig. 7, which requires a low-loss delay line to be efficient (say 80%).

#### ENERGY PULSE COMPRESSION AND MULTIPLICATION

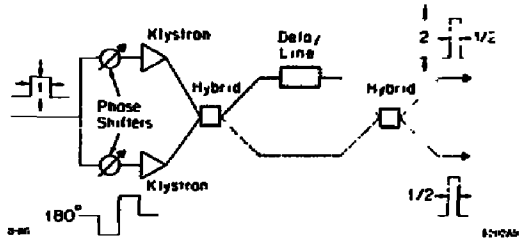


Fig. 7. Single stage of an energy pulse compression and multiplication scheme.

Assuming somehow that the peak powers required are achievable, let us refer to Fig. 8 which summarizes all the efficiencies in the present SLAC RF system. We see that the

#### PRESENT SLAC RF SYSTEM EFFICIENCIES

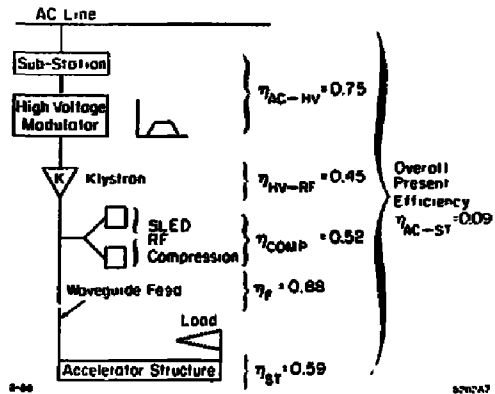


Fig. 8. Present efficiencies of individual sub-systems and of global RF system used for the SLC.

global efficiency  $\eta_{AC-ST}$  from the AC line to storage in the accelerator is less than 10%. Assuming that  $\eta_{ST-B}$  could be made as high as 10%, this would only provide an overall efficiency of 1%, i.e., the AC power to the machines shown in Table 1 would be 100 times higher than  $P_B$ . Thus, whatever scheme in Fig. 3 is considered, it will have to be judged at least

in part on its  $\beta_{AC} \sim \beta_T$  efficiency. For the 10 TeV machine, a number of 30% would be desirable. Achieving this will require a large amount of research and optimisation.

### Wakefields, Single Bunches and Multiple-Bunch Trains

The subject of wake fields in linac structures is too lengthy to be treated here in detail. As is well known, these fields are measured in terms of wake potentials<sup>15</sup> which give the voltage and transverse kick vs. time produced by a unit charge delta function traversing one periodic length of structure. The longitudinal wake potential scales as  $\omega^2$  and the dipole wake as  $\omega^3$ .

The transverse emittance growth in the future machines will have to be controlled drastically by minimising position and angular injection jitter, by probably increasing the focusing strength of the lattice above SLC specifications (presently  $\beta_{max} \sim 10$  m,  $\beta_{min} \sim 2$  m at injection), perhaps by using permanent magnets, by controlling misalignments and vibrations of accelerator sections and quadrupoles to a few microns or less, and by using Landau damping.<sup>19</sup>

The energy spread due to the longitudinal wake fields can be cancelled completely<sup>20</sup> by properly shaping the longitudinal charge distribution of the bunch and by placing its head at a specified angle  $\theta_0$  with respect to the crest of the accelerating wave: the net voltage induced by the wake fields is made to cancel exactly the rising slope of the sine wave where the bunch is placed. Figure 9 shows examples of five such bunch shapes and their respective head positions ( $\theta_0$ ) that have been calculated for zero energy spread in the SLC. The case where  $\theta_0 = 15.5^\circ$  is very close to a truncated Gaussian, thus not too

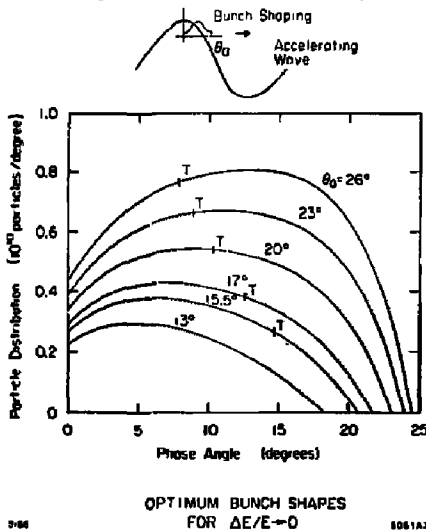


Fig. 9. Examples for the SLC structure of five bunch shapes, each starting with the bunch head at a given angle  $\theta_0$ , for total energy spread cancellation within the bunch. The letter "T" designates the point where the integrated charge in the bunch reaches  $5 \times 10^{10} e^-$ . Note that for the  $\theta_0 = 13^\circ$  case, the shape is such that the bunch cannot reach this charge.

difficult to realize physically. Note however that with the low values of  $N$  shown in Table 1, the constraints on  $\sigma_z$  and the high gradients desirable, it may not be possible, even in theory, to achieve the proper bunch charge distribution, let alone to obtain it in practice from an injector or damping ring and RF compressor. At high gradients, the  $\Delta E/E$  is more likely to be dominated by the bunch length and be on the order of  $\frac{1}{2}(\sigma_z/\lambda)^2$ , which probably will be acceptable for the final focus as long as it remains within less than  $\frac{1}{2}\%$ . We showed earlier, however, that to keep the overall efficiency within acceptable bounds, we would need to accelerate several (maybe on the order of 10) bunches per RF pulse. Several approaches are possible.<sup>18</sup> One is to use traveling-wave structures as illustrated in Fig. 10(a) in such a way that all bunches acquire roughly the same energy: the bunch train of duration  $t_B$  is injected at  $t = t_F - t_B$  when the "missing" voltage  $\Delta V = V[2r/(e^{2r} - 1)]t_B/t_F$  is equal to the voltage eventually removed by the  $b$  bunches ( $bN\sigma_e t/2$ ). This scheme can be used in conjunction with a layout of several interaction points as shown in Fig. 11(a). Note that for  $r = 0.37$ ,  $\Delta V/V \sim t_B/2t_F$ . If for example we want 5% of the energy stored to be removed, then  $t_B/t_F$  must be equal to 0.05, which results in a  $t_B$  of 40 nsec for a SLC-type section. Thus, for  $b = 10$ , the bunch separation would be 4 nsec, or 120 cm. With the filling time dropping as  $\omega^{-3/2}$ , this bunch interval would for example decrease to 500 ps at four times the SLC frequency. It remains to be seen if this will be acceptable from the point of view of transverse wake fields (i.e. bunch-to-bunch deflections) and to the experimenters. Another approach is to lengthen the RF pulse to  $t_F + t_B$  and to inject the bunch train at  $t = t_F$ , in which case successive bunches are separated in energy and a layout as shown in Fig. 11(b) may be used. Similar approaches with standing-wave structures are also possible [Fig. 10(b)].

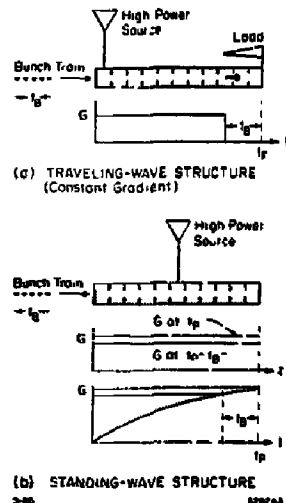


Fig. 10. Multibunch injection for traveling-wave and standing-wave structures to minimise energy difference between bunches.

## Conclusions

An attempt has been made in this paper to present a number of the problems facing the designers of future linear colliders, as well as to describe some of their solutions. Up to the 1 TeV level, it should be possible to use one of the proposed RF approaches described in this paper, although the achievement of the required peak powers and overall system efficiencies still remains to be proven. A considerable R&D effort will also have to be mounted to establish the feasibility of damping rings capable of producing bunches with the required invariant emittance and length, of linacs through which these quantities are preserved, and of final foci giving the required  $\beta^*$  at the interaction points. Reaching the 10 TeV level presents an even greater challenge. The problem of energy spread due to beamstrahlung must first be clarified. Then, undoubtedly, new technologies will have to be invented to produce the required acceleration and six-dimensional beam phase space.

### POSSIBLE LAYOUTS FOR THE BEAM SWITCHYARDS (BSY), FINAL FOCI (FF) AND INTERACTION POINTS (IP)

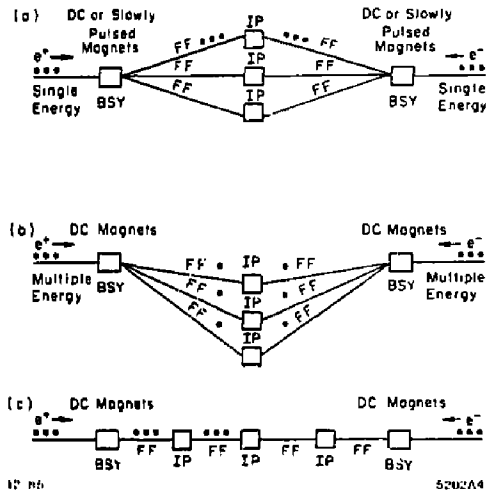


Fig. 11. Possible layouts for the beam switchyards, final foci and interaction points in a high energy  $e^+e^-$  linear collider: (a) train of bunches of equal energies directed to one of several parallel interaction points; (b) train of bunches of different energies directed to several parallel interaction points; (c) train of bunches of similar energies directed to one of several interaction points in series.

## Acknowledgements

The author wishes to thank Juwen Wang, Roger H. Miller and Perry B. Wilson for useful discussions and contributions.

## References

1. P. B. Wilson, "Future  $e^+e^-$  Linear Colliders and Beam-Beam Effects," presented at the 1986 Linear Accelerator Conference, SLAC, June 1986, SLAC-PUB-3985.

2. W.K.H. Panofsky, "Beam Dynamics Parametrisation," SLAC/AAS Note-13, January 1966.
3. R. B. Palmer, "Cooking Rings for TeV Colliders," SLAC-PUB-3883, February 1986.
4. W. M. Fawley, et al., "Novel Accelerators Employing High-Current Electron Beams: Numerical Simulations," presented at the 1986 Linear Accelerator Conference, SLAC, June 1986.
5. W. Schnell, "A Two-Stage RF Linear Collider Using a Superconducting Drive Linac," CERN-LEP-RF/86-06, February 1986.
6. A. M. Sessler and D. B. Hopkins, "The Two-Beam Accelerator," presented at the 1986 Linear Accelerator Conference, SLAC, June 1986.
7. U. Amaldi and C. Pellegrini, "Linear Colliders Driven by a Superconducting Linac-FEL System," CERN/CLIC-Note 16, June 1986.
8. G. A. Voss, et al., "Wake Field Acceleration," presented at the 1986 Linear Accelerator Conference, SLAC, June 1986.
9. P. B. Wilson, "Wake Field Accelerators," SLAC-PUB-3891, February 1986.
10. W. Willis, "Switched Power Linac," AIP Conf. Proc. No. 130 Laser Acceleration of Particles, p 421-434, Malibu, CA, 1985.
11. F. Villa, "High Gradient Linac Prototype: A Modest Proposal," SLAC-PUB-3875, January 1986.
12. The use of elastance for the ratio  $G^2/W$  was suggested by Z. D. Farkas, see IEEE Trans. Nucl. Sci., NS32, No. 5, 3225 (1985).
13. J. W. Wang et al., "RF Breakdown Studies in a SLAC Disk-Loaded Structure," presented at the 1986 Linear Accelerator Conference, SLAC, June 1986, SLAC-PUB-3940.
14. E. Tanabe et al., "Voltage Breakdown at X-Band and C-Band Frequencies," presented at the 1986 Linear Accelerator Conference, SLAC, June 1986.
15. P. B. Wilson, "Linear Accelerators for TeV Colliders," SLAC-PUB-3674, May 1985.
16. G. A. Loew, "Some Issues Involved in Designing a 1 TeV (c.m.)  $e^+e^-$  Linear Collider Using Conventional Technology," SLAC-PUB-3892, February 1986.
17. Z. D. Farkas et al., "SLED: A Method of Doubling SLAC's Energy," Proc. of the IXth Int. Conf. on High Energy Accelerators, May 1974, p 576.
18. Z. D. Farkas et al., "Binary Power Multiplier," SLAC-PUB-3694.
19. K.L.F. Bane, "Landau Damping in the SLAC Linac," SLAC-PUB-3670, May 1985.
20. G. A. Loew and J. W. Wang, "Minimising the Energy Spread Within a Single Bunch by Shaping Its Charge Distribution," SLAC-PUB-3598, October 1985.

## **DISCLAIMER**

This report was prepared as an account of work sponsored by an agency of the United States Government. Neither the United States Government nor any agency thereof, nor any of their employees, makes any warranty, express or implied, or assumes any legal liability or responsibility for the accuracy, completeness, or usefulness of any information, apparatus, product, or process disclosed, or represents that its use would not infringe privately owned rights. Reference herein to any specific commercial product, process, or service by trade name, trademark, manufacturer, or otherwise does not necessarily constitute or imply its endorsement, recommendation, or favoring by the United States Government or any agency thereof. The views and opinions of authors expressed herein do not necessarily state or reflect those of the United States Government or any agency thereof.